

Chemical Nature of Superhydrophobic Aluminium Alloy Surfaces Produced via a One-Step Process Using Fluoroalkyl-Silane in a Base Medium

N. Saleema*†‡, D. K. Sarkar‡, D. Gallant†, R. W. Paynter§, and X.-G. Chen‡

† Aluminum Technology Centre, National Research Council of Canada (ATC-NRC), 501 Boulevard University East, Saguenay, Quebec G7H 8C3 Canada

‡ Centre Universitaire de Recherche sur l'Aluminium (CURAL), University of Quebec at Chicoutimi (UQAC), 555 Boulevard University East, Saguenay, Quebec G7H 2B1 Canada

§ INRS-ÉMT, 1650 Boulevard Lionel-Boulet, Varennes, Québec J3X 1S2 Canada

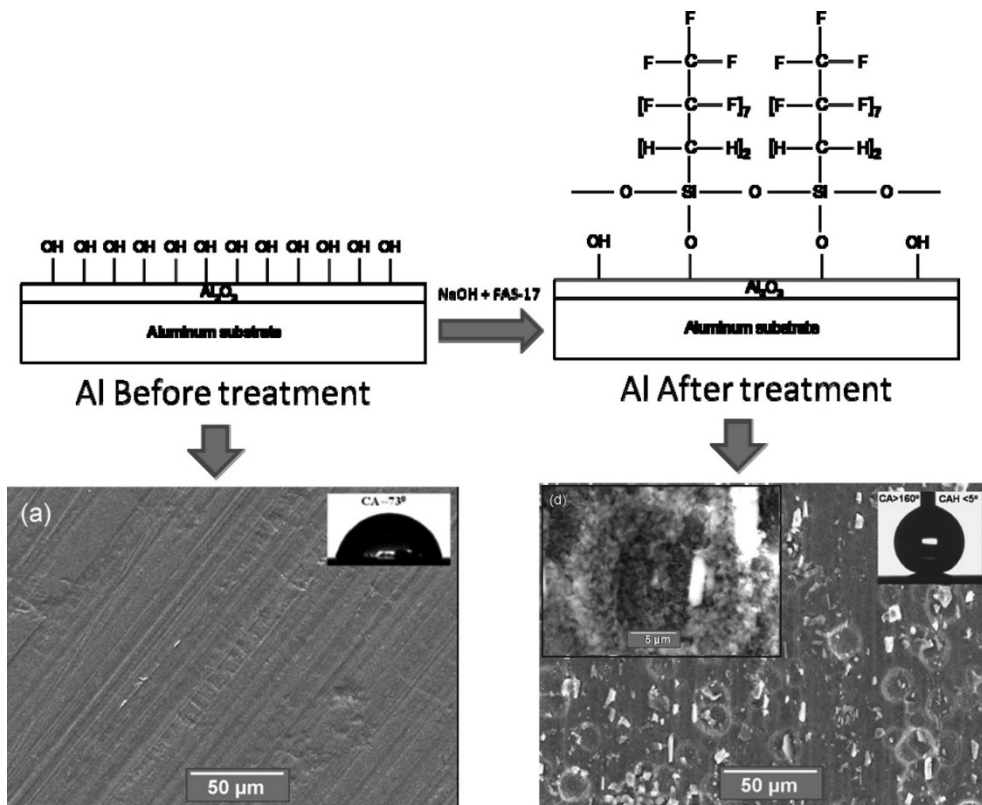
ACS Appl. Mater. Interfaces, **2011**, 3 (12), pp 4775–4781

DOI: 10.1021/am201277x

Publication Date (Web): November 23, 2011

*Tel.: (418) 545-5246. Fax: (418) 545-5345. E-mail: saleema.noormohammed@imi.cnr-nrc.gc.ca.

Abstract



Various surface characterization techniques were used to study the modified surface chemistry of superhydrophobic aluminum alloy surfaces prepared by immersing the substrates in an aqueous solution containing sodium hydroxide and fluoroalkyl-silane (FAS-17) molecules. The creation of a rough micronanostructure on the treated surfaces was revealed by scanning electron microscopy (SEM). X-ray photoelectron spectroscopy (XPS) and infrared reflection absorption spectroscopy (IRRAS) confirmed the presence of low surface energy functional groups of fluorinated carbon on the superhydrophobic surfaces. IRRAS also revealed the presence of a large number of OH groups on the hydrophilic surfaces. A possible bonding mechanism of the FAS-17 molecules with the aluminum alloy surfaces has been suggested based on the IRRAS and XPS studies. The resulting surfaces demonstrated water contact angles as high as $\sim 166^\circ$ and contact angle hystereses as low as $\sim 4.5^\circ$. A correlation between the contact angle, rms roughnesses, and the chemical nature of the surface has been elucidated.

Keywords : superhydrophobic aluminum alloy; contact angle; surface roughness; scanning electron microscopy (SEM); X-ray photoelectron spectroscopy (XPS); infrared reflection absorption spectroscopy (IRRAS); profilometry

Introduction

Superhydrophobic surfaces find tremendous importance in fundamental research because of their potential usefulness in key industries. Superhydrophobicity exists inherently on the surfaces of many natural tissues, plants, and animal bodies. One of the most classic examples is the lotus leaf surface, which has inspired researchers around the world because of its self-cleaning and water-repellent properties. The key element in water repellency on lotus leaf surfaces is the presence of a low surface energy hydrophobic surface coating composed of epicuticular wax crystals on a microscopically rough structure.⁽¹⁾ Because of the importance of superhydrophobic surfaces in today's emerging technologies, many efforts have been made to replicate nature. The term "biomimicking" is commonly used to denote the artificial production of superhydrophobic surfaces. Because of their unique water-repellency and self-cleaning abilities, the applications of superhydrophobic surfaces are diverse and include areas such as corrosion resistance, stain-resistant textiles, drag-reduction, inhibition of snow or ice adhesion, biomedical applications, anti-biofouling paints for boats, bio-chips, eyeglasses, and self-cleaning windshields for automobiles.⁽²⁻¹¹⁾ We have previously shown that superhydrophobic aluminum surfaces prepared using a two-step process by chemically

etching aluminum surfaces and further coating with ultrathin films of Teflon by rf-sputtering demonstrated excellent icephobic properties.(7, 8)

Traditionally, superhydrophobic surfaces are made by combining two steps that involve the creation of a rough micronanopattern in the first step and the passivation of the rough surface using a low surface energy coating to lower the surface energy in the second step.(7, 8, 12-15) The combined effect of air entrapment in the rough micronanostructures and the low surface energy reduces the affinity of water toward the surface. We have previously reported several superhydrophobic surfaces prepared via two-step procedures where rough micronanostructures were created via techniques such as chemical bath deposition (CBD), substrate chemical etching, galvanic exchange reactions, etc. The passivation of these surfaces was carried out using organic molecules such as stearic acid, fluoroalkyl-silane (FAS-17) molecules, or by coating with rf-sputtered Teflon.(12-15) All these studies emphasized the importance of the coexistence of both surface roughness and the low surface energy coating in order for the surface to exhibit superhydrophobicity.

On the other hand, we have also reported the preparation of superhydrophobic surfaces of aluminum alloy, silver nanostructures, etc., via a one-step procedure in which both the creation of a rough micronanostructure and the lowering of the surface energy take place simultaneously in one single step.(16-18) In the present study, aluminum alloy surfaces are rendered superhydrophobic using a simple one-step process in which the aluminum coupons are simply immersed in an aqueous solution containing FAS-17 molecules and sodium hydroxide (NaOH). The SEM studies reveal the creation of a rough micronanopattern on the treated surfaces and the XPS and IRRAS studies confirm the presence of FAS-17 molecules. An attempt has also been made to investigate the corrosion behavior of superhydrophobic aluminum surfaces in comparison with their hydrophilic counterparts.

Experimental Details

Aluminum alloy coupons (AA6061 alloy), 1" × 1", were ultrasonically degreased in 1% Liquinox solution for 10 min followed by ultrasonication with deionized water, twice for 10 mins each time. The clean Al coupons were simply immersed in beakers containing a mixture of varying concentrations (0.1–0.8 M) of sodium hydroxide (NaOH) and 0.1 M fluoroalkyl-silane ($\text{CH}_3(\text{CF}_2)_7(\text{CH}_2)_2\text{Si}(\text{OC}_2\text{H}_5)_3$) at varying FAS-17 to NaOH molar ratios and placed in an ultrasonic bath for varying time periods (5–25 min). All the treated

coupons were rinsed in deionized water and dried in air for several hours prior to further characterization. The morphological analysis was performed using a scanning electron microscope (SEM, JEOL JSM 6480 LV). The root mean square (rms) roughness of the resulting surfaces was measured using an AD phase shift optical profilometer. Infrared reflection absorption spectroscopy (IRRAS) and X-ray photoelectron spectroscopy (XPS) were employed to characterize the surface chemistry of the resulting surfaces. IRRAS (Nicolet 6700 FT-IR) is equipped with a Mid-IR MCT-A N₂-cooled detector and a KBr beam splitter. The Smart SAGA (specular apertured grazing angle) accessory was used to analyze samples at an average incidence angle of 80° relative to the normal surface. The spectra were recorded from 4000 to 650 cm⁻¹ with a resolution of 4 cm⁻¹ and 120 scans. The IR radiation was p-polarized, and the resulting spectrum was subtracted from a background spectrum taken from a clean gold-coated reference sample. The XPS (VG ESCALAB 220iXL) survey and high resolution core level spectra were collected by using an Al K α (1486.6 eV) X-ray source. All the samples were tested for superhydrophobicity using a contact angle goniometer (Krüss GmbH, Germany). The advancing and receding contact angles were measured by fitting images of the asymmetric water drops using the tangent-2 method, with Krüss DSA software.⁽¹⁹⁾ The difference between the advancing and receding contact angles is the contact angle hysteresis. The corrosion resistance of the samples was investigated via the potentiodynamic polarization curves acquired by immersing the samples in a 3.5% NaCl solution (natural pH 5.9) for a duration of 24 h. Electrochemical experiments were performed using a Reference 600 potentiostat (Gamry Instruments, Warminster, PA, USA) and a 300 cm³ - EG&G PAR flat cell (London Scientific, London, ON, Canada), equipped with a standard three-electrode system with an Ag/AgCl reference electrode, a platinum mesh as the counter electrode (CE), and the sample as the working electrode (WE).

Results and Discussion

A chemical reaction of NaOH with aluminum in presence of FAS-17 molecules results in an etching process due to the presence of NaOH in the solution leading to a rough microporous micro-nanostructure on the surfaces as shown in the FESEM images of Figure 1. Figure 1b–d shows the aluminum surfaces treated with NaOH in the presence of FAS-17 molecules at a FAS-17/NaOH ratio of 0.2, revealing craterlike microfeatures of ~10 μm in size, evolved following treatment, as compared to the as-received clean aluminum surface shown in Figure 1 (a). The microcraters are in addition decorated with

nanometer sized fibers as is evident from the higher magnification images shown in Figure 1c,d, which are also present all over the surface providing the system with a two-tier micro-nano binary structure. The presence of such a rough binary structure on a surface is one of the two important requirements for superhydrophobicity.(1, 12-18) Further SEM analyses also revealed that these morphological features remained similar on all surfaces treated with FAS-17 molecules. We have previously reported microcrater formation on surfaces treated with NaOH and FAS-17.(16) Fu and He also reported a binary structure composed of microscale crater-like pits and nanoscale reticula on aluminum surfaces, but via a two-step roughening procedure which involved metallographic abrasion followed by etching in a combination of nitric acid and copper nitrate.(20) The formation of a rough binary microcratered nanofibrous structure on the surface in combination with a modified chemistry arising from the adhesion of low surface energy FAS-17 molecules, contributes to the evolution of superhydrophobic properties.

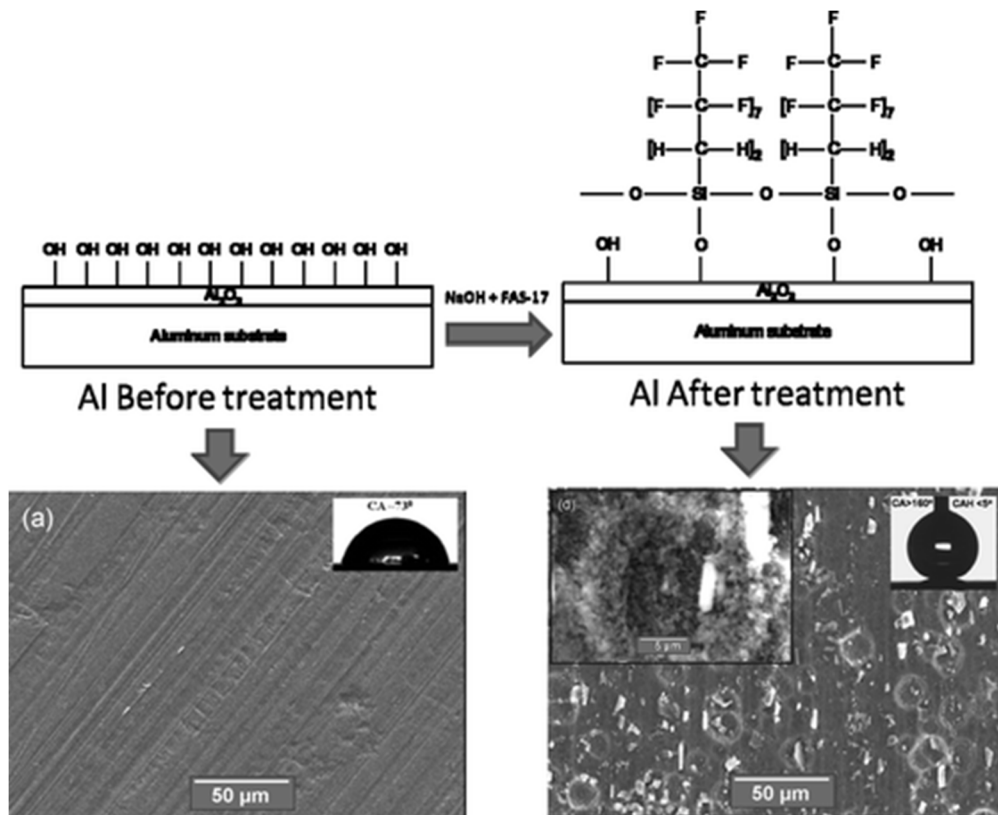


Figure 1. SEM images of (a) untreated aluminum; (b) aluminum treated with NaOH and FAS-17 with a (FAS-17/NaOH) molar ratio of 0.2 for 15 min; (c) and (d) higher-magnification images of b.

IRRAS spectral analysis of the aluminum surfaces treated with NaOH and FAS-17 at different FAS-17/NaOH molar ratios and for different treatment times, recorded in the wavenumber range of 4000–650 cm^{-1} (see the [Supporting Information](#) for full range IRRAS spectra) revealed the presence of the fluorinated functional groups which are mainly responsible for the lowering of surface energies. The –OH stretching absorption bands centered in the wavenumber range of 3600–3000 cm^{-1} arising from aluminum hydroxide formed on the surface following a reaction during etching was observed in the full range IR spectra.(21, 22) Al Abadleh and Grassian have presented similar hydroxide IR peaks for water adsorption on alumina powder.(21) Figure 2a shows the IR spectra of the aluminum alloy surfaces treated with a FAS-17/NaOH ratio of 0.2 for different treatment periods in the wavenumber range of 1800-650 cm^{-1} . The appearance of peaks belonging to –CF₂– functional groups arising from C–F stretching vibration are evident in all these spectra between wavenumbers of 1120 and 1350 cm^{-1} .(23-25) It can be seen that the intensity of these peaks is at its maximum at 15 minutes of treatment time. Therefore, a critical etching time of 15 minutes has been encountered after which the peak intensities slightly decreased with further increase in the time of treatment.

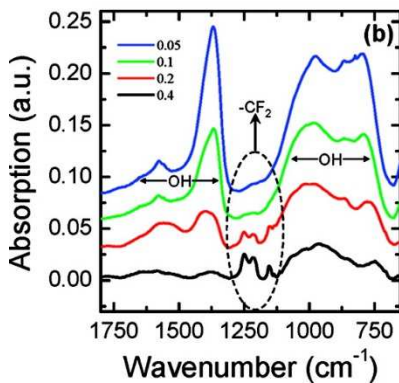
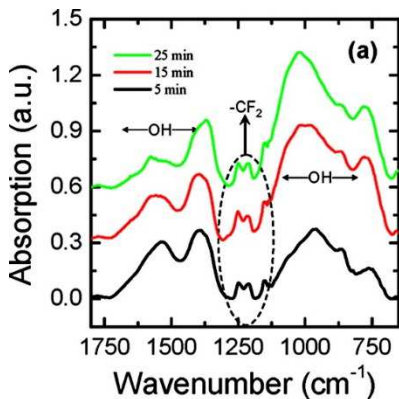


Figure 2. IRRAS spectra acquired on aluminum alloy surfaces treated (a) with a FAS-17/NaOH molar ratio of 0.2 for different treatment times and (b) with different FAS-17/NaOH molar ratios for 15 min treatment time.

Figure 2b shows the IR spectra of the surfaces treated with varying molar ratios of FAS-17 to NaOH (0.05–0.4) for the critical etching time of 15 min obtained from the time-dependent studies. The peaks belonging to $-\text{CF}_2-$ functional groups emerge between the wavenumbers of 1120 and 1350 cm^{-1} ; (23-25) however, these peaks are present only on the surfaces treated with FAS-17/NaOH ratios of 0.4 and 0.2, with increased intensity of the peaks for the surface treated with the higher FAS-17/NaOH ratio of 0.4. These C–F stretching vibrations disappear as the FAS-17/NaOH ratio further decreases to 0.1 and 0.05. Therefore, a higher relative concentration of NaOH in the solution slows down the deposition of the FAS-17 molecules onto the aluminum alloy surface during the reaction. In both time-dependent and concentration-dependent studies, a few other prominent IR peaks are also seen which have a tendency to increase with increasing etching times and decreasing FAS-17/NaOH molar ratios. These peaks are situated around 700–1000, 1370, and 1580 cm^{-1} . The peaks appearing around 1370 and 1580 cm^{-1} may be assigned to the bending mode of molecular water coordinated to octahedral and tetrahedral aluminum ion sites, respectively, on alumina according to Vlaev et al. (6) Other studies indicate that these peaks may originate from adsorbed water on an aluminum oxide surface. (22) The peaks observed between 700–1000 cm^{-1} may also be associated with the hydroxide formed as a result of water adsorption on the aluminum alloy surfaces during the etching reaction. All these peaks are found to increase in intensity with decreasing FAS-17/NaOH ratios. Therefore, with increased NaOH concentrations in the aqueous mixture of NaOH and FAS-17 and with increased treatment times, the water adsorption is greater, increasing the hydroxide group concentration with reduced concentrations of fluorinated functional groups on the surface. Increased amounts of hydroxides and reduced or negligible amounts of low surface energy fluorinated groups on the surface may not lead to superhydrophobic properties.

XPS investigations of the aluminum alloy surfaces treated with NaOH and FAS-17 at different FAS-17/NaOH ratios for 15 min revealed the presence of C, F, O, and Si with no trace of Na present in the survey spectra (see the Supporting Information). Figure 3a, b shows the high-resolution C1s core level spectra with the corresponding O1s spectra in the inset, acquired from the aluminum surface treated with a FAS-17/NaOH ratio of

0.4 and 0.1, respectively. The C1s spectrum of the surface treated with a FAS-17/NaOH ratio of 0.4 was resolved into seven components, namely, $-\text{CF}_3$ (293.82 eV), $-\text{CF}_2$ (291.22 eV), $-\text{CH}_2-\text{CF}_2$ (288.82 eV), $-\text{C}-\text{O}$ (286.14 eV), $-\text{C}-\text{C}$ (284.7 eV), $-\text{C}-\text{Si}$ (281.78 eV), and $-\text{C}-\text{metals}$ (280.81 eV). The C1s spectrum of the surface treated with a FAS-17/NaOH ratio of 0.1 could also be resolved into seven components, namely, $-\text{CF}_3$ (293.6 eV), $-\text{CF}_2$ (291.1 eV), $-\text{CH}_2-\text{CF}_2$ (288.68 eV), $-\text{C}-\text{O}$ (286.5 eV), $-\text{C}-\text{C}$ (284.5 eV), $-\text{C}-\text{Si}$ (281.72 eV), and $-\text{C}-\text{metals}$ (279.5 eV). The F1s peak in both cases was observed at 688.5 eV. The O1s binding energies observed on the surfaces treated with FAS-17/NaOH ratios of 0.4 and 0.1 were 531.8 and 531.1 eV, respectively. The binding energies reported here are consistent with our previous reports.[\(16, 27\)](#)

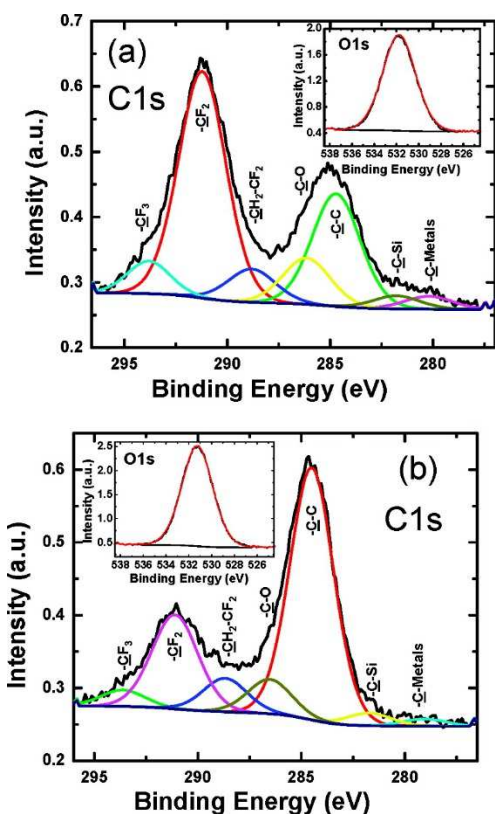


Figure 3. High-resolution C1s core level spectrum Al surfaces treated with a FAS-17/NaOH ratio of (a) 0.4 and (b) 0.1; inset shows the corresponding high-resolution O 1s spectra.

The CF_3 and CF_2 concentrations from the C1s spectra of the surface treated with a FAS-17/NaOH molar ratio of 0.4 is 6.16 and 47.71% as reported previously by us.[\(16, 27\)](#)

These values as previously reported are slightly higher than the theoretical values obtained from the molecular structure of FAS-17 molecules, which are 6 and 41%,

respectively, for CF_3 and CF_2 . The higher concentrations of CF_3 and CF_2 observed on the surface indicate that these low surface energy components comprise the outermost surface, contributing to superhydrophobic properties. However, with a reduced FAS-17/NaOH molar ratio of 0.1, the CF_3 and CF_2 concentrations as obtained from the C1s spectral analysis lowered to 3.59 and 21.8%, respectively. The reduced concentrations of these low-surface-energy components on the surface treated with a FAS-17/NaOH ratio of 0.1 is consistent with the FTIR analysis.

From the FTIR and XPS investigations, a possible mechanism for the treatment with NaOH and FAS-17 molecules with varying FAS-17/NaOH ratios can be outlined. Figure 4 shows a schematic presentation of possible reaction mechanisms leading to a superhydrophobic surface and a hydrophilic surface. On a surface treated with higher FAS-17/NaOH ratios (for example, a FAS-17/NaOH ratio of 0.2), the formation of aluminum hydroxide and the integration of CF_2 functional groups originating from FAS-17 molecules on the surface as revealed by the FTIR and XPS measurements may be schematized as shown in Figure 4a. The C_2H_5 component is removed from FAS-17 molecules in the hydrolysis process and the silicon bonds with the oxygen in the surface so that the C–F functional groups are oriented outward from the surface. Such a bonding does not take place throughout the surface as evidenced by the observation of a few OH groups on the surface. The number of FAS-17 molecules adhered to the surface with the low surface energy C–F functional groups oriented outward on the resulting surface may be sufficient to provide superhydrophobic properties. However, when the FAS-17/NaOH ratio is lower, the etching of the surface dominates over the integration of FAS-17 molecules. Therefore, the resulting surface is characterized by a large number of OH groups with a negligible concentration of FAS-17 molecules present as revealed by IRRAS measurements, schematized in Figure 4b. The presence of a large number of OH groups on the surface may lead to hydrophilic behavior as the affinity of water is higher with hydroxides.

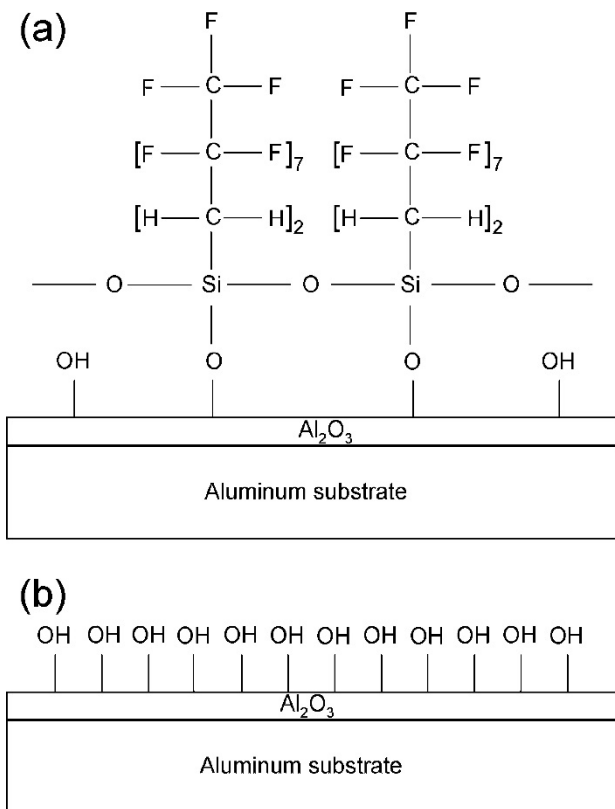


Figure 4. Schematic of bonding mechanism of FAS-17 molecules on (a) superhydrophobic and (b) hydrophilic aluminum alloy surface.

Figure 5a, b shows the variation in the water contact angle and rms roughness, respectively, with treatment time for surfaces treated with a FAS-17/NaOH ratio of 0.2. It is clear from Figure 5a that with increasing time the contact angle increases up to a critical etching time of 15 min and then begins to decrease. A water contact angle value of only $146 \pm 8^\circ$ at 5 min treatment time increased to $161 \pm 6^\circ$ at 15 min treatment time, combined with a very low contact angle hysteresis of $5 \pm 3^\circ$, at which point the water drops started to roll off the surface. Such a high water contact angle can be attributed to the presence of a high concentration of low surface energy fluorinated molecules on these surfaces as revealed by the IRRAS and XPS investigations (Figures 2 and 3). The contact angle hysteresis for surfaces treated for less than 15 min was not possible to measure as the water droplet stuck to those surfaces, demonstrating very low water contact angle values. At a treatment time of 25 min, the surface exhibited a lower water contact angle of $154 \pm 2^\circ$ and a contact angle hysteresis of 14° , remaining in the superhydrophobic zone ($>150^\circ$). Figure 5b shows that the rms roughness of the surfaces increases with treatment time. The rms roughness increased to $0.7 \pm 0.07 \mu\text{m}$ at 15 min treatment time from a value of $0.5 \pm 0.06 \mu\text{m}$ obtained at 5 min treatment time. Along

with increasing rms roughness, the contact angle also increased up to 15 min treatment time. With further increase in treatment time, the rms roughness further increases to a value of $1.2 \pm 0.1 \mu\text{m}$ at 25 min treatment time, however, the water contact angle value starts to decrease. This reduction in water contact angle in spite of higher rms roughness may be due to the loss of CF_2 fragments at longer etching times; eventually leading to more hydroxide on the surface as revealed by FTIR studies (Figure 2a). Therefore, it may be concluded that a critical time of treatment of 15 minutes is necessary to obtain superhydrophobic properties after which the superhydrophobic behavior is found to gradually deteriorate.

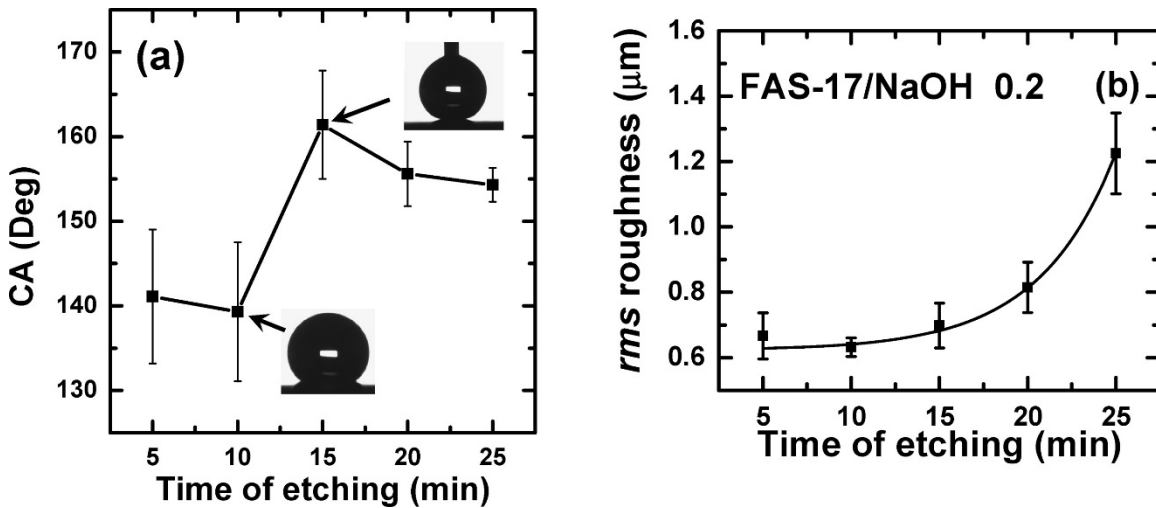


Figure 5. (a) Water contact angle measured on aluminum alloy surfaces and (b) surface roughness of aluminum alloy surface as a function of the etching time, treated with a FAS-17/NaOH molar ratio of 0.2.

Figure 6a, b shows the variation in the water contact angle and rms roughness, respectively, on the aluminum alloy surfaces treated with different FAS-17/NaOH ratios for a treatment period of 15 min. Figure 6a shows an increase in the water contact angles with increasing FAS-17/NaOH ratio. Below a FAS-17/NaOH ratio of 0.2, the surfaces were found to be hydrophilic with the water contact angle values below 90° . Superhydrophobic behavior was obtained when the FAS-17/NaOH ratio was 0.2 with a very high water contact angle of $161 \pm 6^\circ$ and very low contact angle hysteresis of $5 \pm 3^\circ$. With further increase in the FAS-17/NaOH ratio to 0.4, the water contact angle further increased to $166 \pm 4.5^\circ$ and the contact angle hysteresis further decreased to $4 \pm 0.5^\circ$. Therefore, a FAS-17/NaOH ratio of 0.2 is found to be the critical concentration necessary to obtain superhydrophobic properties on the aluminum alloy surfaces. The increase in water contact angles, again, can be attributed to the presence of low-

surface-energy C–F functional groups on the surface oriented outward from the surface (Figure 4) as revealed by the IRRAS and the XPS investigations. However, Figure 6b shows that the rms roughness decreases with increasing FAS-17/NaOH ratios. Below the critical FAS-17/NaOH ratio of 0.2, the rms roughness varied between 1.6 and 2.3 μm . The rms roughness remained similar with values of $0.75 \pm 0.07 \mu\text{m}$ and $0.7 \pm 0.06 \mu\text{m}$, respectively, on surfaces treated with FAS-17/NaOH ratios of 0.2 and 0.4. It is clear from these values that with higher rms roughness, the contact angle values are lower and in the hydrophilic zone and with lower roughness, the contact angle values are higher and in the superhydrophobic zone. The lower contact angles on the surfaces with higher rms roughness can be attributed to the presence of a higher concentration of hydroxides on these surfaces as is evident from the IRRAS studies (Figure 2b). Lower FAS-17 to NaOH ratios lead to a surface modification dominated by roughening of the surface, and also resulting in the fragmentation of FAS-17 molecules, as seen by XPS, leading to a negligible coverage by low surface energy fluorinated compounds on the surface. However, the higher contact angles on the surfaces with a lower *rms* roughness of $\sim 0.7 \mu\text{m}$ treated with higher FAS-17 to NaOH ratios indicate that this roughness is sufficient to obtain superhydrophobicity provided that a sufficient number of low surface energy components are correctly oriented on the surface. Generally, an increase in roughness of a surface while maintaining a constant low surface energy leads to large amount of air entrapment resulting in an increase in water contact angle values according to Cassie-Baxter model.(28) We have confirmed this behavior in our recent works on FAS modified silica nanoparticles deposited thin films as well as on electrochemically stearic acid modified copper microdots deposited aluminum surfaces.(29, 30) Brassard et al. showed increased water contact angle values on low surface energy FAS modified silica nanoparticles deposited aluminum surfaces where the surface roughness increased due to the increase of particle sizes of the silica nanoparticles.(29) Similarly, Huang et al created the surface roughness by depositing copper microdots on aluminum surface and further modified those copper microdots electrochemically using stearic acid to maintain similar surface chemical composition.(30) Both works showed that increase in surface roughness leads to superhydrophobicity provided the chemical composition of the surface remained same. In contrast to our present work, a higher roughness resulted from an increased NaOH quantity in the solution of FAS-17 and NaOH leads to a reduced water contact angle values. In this present case, we not only increase the surface roughness, but a change

in FAS-17 molecules with loss of CF_3 and CF_2 molecules also occurs as evidenced by XPS. Although higher surface roughness is created in this process, because of the loss of the low-surface-energy components, we obtain lower water contact angles, which contradicts the conventional thought.

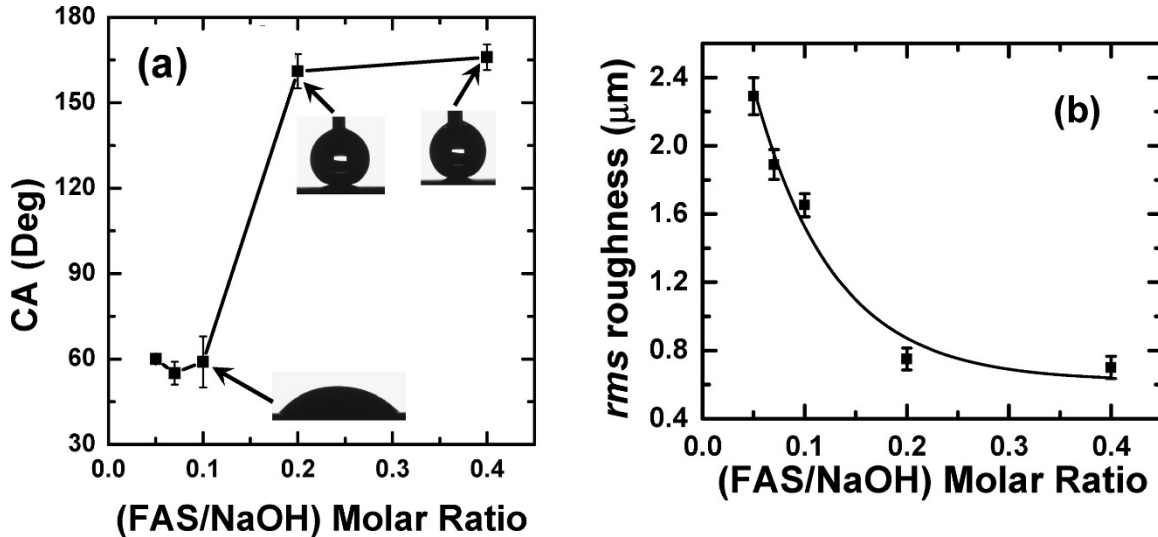


Figure 6. (a) Water contact angle measured on aluminum alloy surfaces and (b) surface roughness of aluminum alloy surfaces treated with different FAS-17/NaOH molar ratios for 15 min etching time.

We have previously reported similar high water contact angles and low contact angle hystereses on various surfaces produced via one-step as well as two-step processes.^(12, 13, 16, 17) Sarkar et al. reported a water contact angle of $164 \pm 3^\circ$ and a hysteresis of $2.5 \pm 1.5^\circ$ via a two-step process on chemically etched aluminum surfaces coated with rf-sputtered Teflon.⁽¹³⁾ Fu and He's study on superhydrophobic aluminum surfaces produced by a combination of mechanical abrasion and chemical etching followed by passivation with decyl-triethoxysilane demonstrated a similar water contact angle of 159.7° .⁽²⁰⁾ Song and Shen reported a contact angle of 150° on aluminum sheets exhibiting a petal-like microstructure via a two-step procedure of surface roughening by immersion in a chemical solution of $\text{NH}_2(\text{CH}_2)_6\text{NH}_2$ followed by passivation using perfluorodecyltriethoxysilane.⁽³¹⁾ All these authors, however, reported superhydrophobic aluminum surfaces produced via a two-step procedure involving surface roughening methods to obtain a rough micro-nanostructure and surface passivation methods to lower the surface energy. In the present study, we have reported very high water contact angles ($>160^\circ$) and very low contact angle hystereses ($<5^\circ$) via a

simple one-step procedure in which the creation of a micro-nanoroughness as well as lowering of the surface energy takes place simultaneously. Further, the water contact angle obtained on an as-received aluminum surface of only $73 \pm 3^\circ$, shows that these superhydrophobic surfaces (FAS-17/NaOH > 0.2, rms roughness < 0.7 μm) follow the Cassie-Baxter model where due to the presence of air in the gaps of the rough surface, therefore forming a composite surface of air and the solid, the water contact angle is enhanced to values greater than 150° .⁽²⁸⁾ On the other hand, on the hydrophilic surfaces (FAS-17/NaOH < 0.1, rms roughness > 1.6 μm), the water contact angles drop below 70° , indicating that these surfaces follow Wenzel regime.⁽³²⁾ Therefore, a transition from Wenzel regime to Cassie-Baxter regime has been encountered depending on the FAS-17/NaOH ratio and the corresponding roughness resulting from a certain etching time.

The corrosion behavior of the superhydrophobic aluminum alloy surface (FAS-17/NaOH ratio of 0.2 for 15 min) and the surface treated without FAS-17 molecules was investigated via polarization curves (figure not shown) and FESEM measurements following an immersion of these surfaces in 3.5% NaCl solution for 24 h. The corrosion current densities and the polarization resistance of the hydrophilic surface and the superhydrophobic surface do not show significant difference in their corrosion performance. The coverage of FAS-17 molecules adhered to the aluminum alloy surface may not be, therefore, sufficient to inhibit corrosion significantly as the corrosion current densities of the two surfaces remain practically the same. However, the FESEM images, shown in Figure 7, of the corroded areas of these two surfaces demonstrates that there is a substantial improvement in the corrosion properties as the corrosion pits density is significantly lower on the corroded superhydrophobic surface (Figure 7b) as compared to that of the hydrophilic one (Figure 7a) where the pits are distributed all over the exposed area.

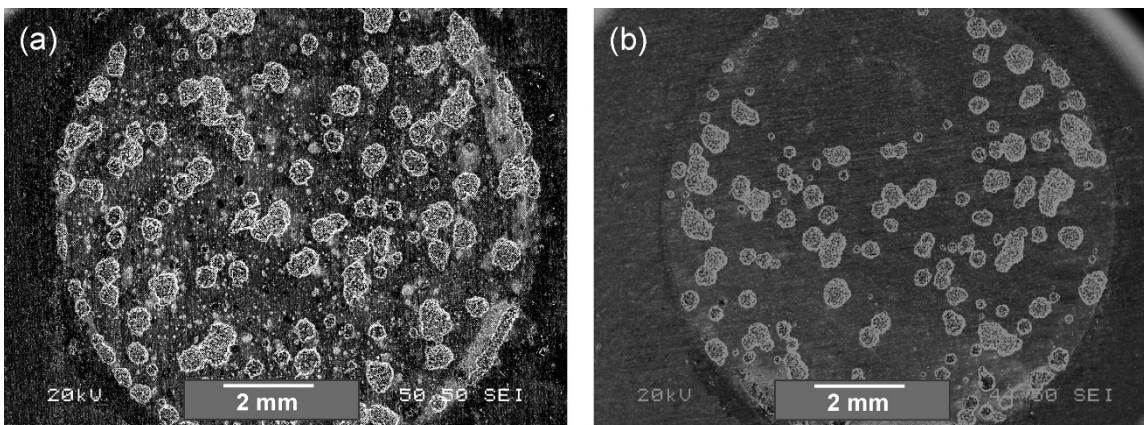


Figure 8. SEM images of corroded surfaces of surface treated with FAS-17/NaOH ratio molar ratio of (a) 0 (hydrophilic) and (b) 0.2 (superhydrophobic).

Conclusion

Highly superhydrophobic aluminum alloy surfaces have been prepared via a very simple one-step technique by immersing the substrates in an aqueous solution of NaOH and FAS-17 molecules. A water contact angle as high as $\sim 166^\circ$ and contact angle hysteresis as low as $\sim 4.5^\circ$ was obtained on the treated surfaces. SEM analysis confirmed the creation of a nanofiber-decorated craterlike binary micro-nanorough structure. IRRAS and XPS analyses confirmed the presence of the low-surface-energy fluorinated components also leading to an understanding of a possible bonding mechanism of FAS-17 molecules with the aluminum alloy surface during the treatment process. The presence of large number of low surface energy fluorinated molecules on the surface has been found to be responsible for the superhydrophobic properties. However, under inappropriate treatment conditions, a negligible concentration of low surface energy components and a large concentration of hydroxides on the surface have been found, resulting in micro-nanostructured surfaces that exhibit hydrophilic behavior.

Supporting information

Survey spectra acquired from aluminum surfaces treated with FAS-17/NaOH ratios of 0.2 and 0.4. IRRAS full range spectra ($4000\text{-}650\text{ cm}^{-1}$). This information is available free of charge via the internet at <http://pubs.acs.org>.

Acknowledgement

We acknowledge the financial support provided by the Natural Sciences and Engineering Research Council of Canada (NSERC). We thank Ms. Y.-M. Han for acquiring the polarization curves at the facilities of Aluminum Technology Centre, National Research Council of Canada (ATC-NRC). We also thank Dr. Stéphan Simard (ATC-NRC) for his critical reading on the manuscript.

References

1. Barthlott, W.; Neihhuis, C. *Planta* 1997, 202, 1
2. Scardino, A.; De Nys, R.; Ison, O.; O'Connor, W.; Steinberg, P. *Biofouling* 2003, 19, 221
3. Singh, A.; Steely, L.; Allcock, H. R. *Polym. Prepr. (ACS, Div. Polym. Chem.)* 2005, 46, 599
4. Gau, H.; Herminghaus, S.; Lenz, P.; Lipowsky, R. *Science* 1996, 283, 46
5. Liu, T.; Yin, Y.; Chen, S.; Chang, X.; Cheng, S. *Electrochim. Acta* 2007, 52, 3709
6. Satoh, K.; Nakazumi, H. *J. Sol-Gel Sci. Technol.* 2003, 27, 327
7. Sarkar, D. K.; Farzaneh, M. *J. Adhesion Sci. Technol.* 2009, 23, 1215
8. Saleema, N.; Farzaneh, M.; Paynter, R. W.; Srakar, D. K. *J. Adhesion Sci. Technol.* 2011, 25, 27
9. Scardino, A.; De Nys, R.; Ison, O.; O'Connor, W.; Steinberg, P. *Biofouling* 2003, 19, 221
10. Samuel, J. D. J. S.; Ruther, P.; Frerichs, H.-P.; Lehmann, M.; Paul, O.; Ruhe, J. *Sens. Actuators, B* 2005, 110, 218
11. Quéré, D. *Rep. Prog. Phys.* 2005, 68, 2495
12. Saleema, N.; Farzaneh, M. *Appl. Surf. Sci.* 2008, 254, 2690
13. Sarkar, D. K.; Farzaneh, M.; Paynter, R. *Mater. Lett.* 2008, 62, 1226
14. Sarkar, D. K.; Farzaneh, M.; Paynter, R. *Appl. Surf. Sci.* 2010, 256, 3698
15. Safaee, A.; Sarkar, D. K.; Farzaneh, M. *Appl. Surf. Sci.* 2008, 254, 2493
16. Saleema, N.; Sarkar, D.K.; Paynter, R.W.; Chen, X.-G. *ACS Appl. Mater. & Interfaces* 2010, 2, 2500
17. Sarkar, D. K.; Saleema, N. *Surf. Coatings Technol.* 2010, 204, 2483
18. Huang, Y.; Sarkar, D. K.; Chen, X. -G. *Mater. Lett.* 2010, 64, 2722
19. Krüss GmbH, DSA1 v1.9-03 (User Manual).
20. Fu, X.; He, X. *Appl. Surf. Sci.* 2008, 255, 1776

21. Al-Abadleh, H. A.; Grassian, V. H. *Langmuir* 2003, 19, 341
22. van den Brand, J.; Van Gils, S.; Beentjes, P.C.J.; Terryn, H.; de Wit, J. H. W. *Appl. Surf. Sci.* 2004, 235, 465
23. Hozumi, A.; Takai, O. *Appl. Surf. Sci.* 1996, 103, 431
24. Takai, O.; Hozumi, A.; Sugimoto, N. *J. Non-Cryst. Solids* 1997, 218, 280
25. Jeong, H.-J.; Kim, D.-K.; Lee, S.-B.; Kwon, S.-H.; Kadono, K. *J. Colloids & Interface Sci.* 2001, 235, 130
26. Vlaev, L.; Damyanov, D.; Mohamed, M.M. *Colloids Surf.* 1989, 36, 427
27. Sarkar, D. K.; Paynter, R. W. *J. Adhesion Sci. Technol.* 2010, 24, 1181
28. Cassie, A. B. D.; Baxter, S. *Trans. Faraday Soc.* 1944, 40, 546
29. Brassard, J. D.; Sarkar, D. K.; Perron, J. *ACS Appl. Mater. Interfaces* 2011, 3, 3583
30. Huang, Y.; Sarkar, D. K.; Chen, X.-G. *Nano-Micro Lett.* 2011, 3, 160
31. Song, H.-J.; Shen, X.-Q. *Surf. Interface Anal.* 2010, 42, 165
32. Wenzel, R. N. *Ind. Eng. Chem.* 1936, 28, 988